Ramsay Maunder ASSOCIATES *Finite Element Specialists and Engineering Consultants*

An equilibrium approach to finite element modelling of plates and shells: with linear and non-linear applications.

Edward Maunder & Bassam Izzuddin

Introduction

This article is based on a presentation given at the first International Conference on Shells, Plates and Beams held in Bologna 9 – 11 September 2015 [1]. The work is a result of recent collaboration between Dr Maunder of Exeter University and Ramsay Maunder Associates, and Professor Izzuddin of Imperial College, London. It concerns hybrid equilibrium flat shell elements governed by Reissner-Mindlin theory and assuming small strains and linear elastic material. These are used to model a simply supported flat plate assuming small displacements, and a cylindrical shell with small or large translations and rotations. Comparisons are made with models composed of curved conforming elements.

The flat shell element is a quadrilateral macro-element assembled from 4 triangular primitive elements so as to control spurious kinematic modes, which act like pseudo-mechanisms.

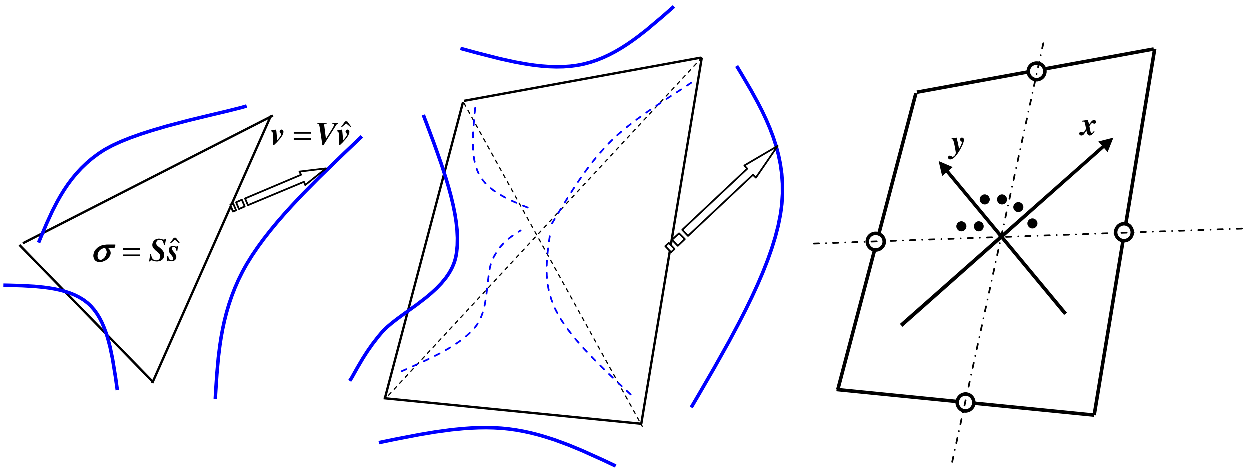

Primitive triangular element

Quadrilateral macro-element

Local Cartesian frame for a macro-element

Figure 1: Hybrid equilibrium element as a macro-element

The hybrid elements are based on statically admissible stress fields $\boldsymbol{\sigma} = \boldsymbol{S}\hat{\boldsymbol{s}}$ defined within each primitive element, and displacement fields $\boldsymbol{v} = \boldsymbol{V}\hat{\boldsymbol{v}}$ defined independently for each side. The columns of $\boldsymbol{S}$ and $\boldsymbol{V}$ represent independent fields, and the vectors $\hat{\boldsymbol{s}}$ and $\hat{\boldsymbol{v}}$ collect the stress and displacement parameters. whether internal or external, as indicated in Figure 1. The assembly of primitive elements into a macro-element effectively condenses out the internal degrees of freedom.

The right hand part of Figure 1 indicates that degrees of freedom, which include the 6 rigid body freedoms of a side, are treated as if focused at the midpoints which serve as structural nodes within the program ADAPTIC [2]. A local stiffness matrix $\boldsymbol{K}\hat{\boldsymbol{v}} = \hat{\boldsymbol{t}}$ for a macro-element is formulated based on weak forms of compatibility of strains (corresponding to the stresses) with side displacements $\hat{\boldsymbol{v}}$, and a strong form of equilibrium between stresses and side tractions $\hat{\boldsymbol{t}}$ [3].

For large displacements with small strains we formulate a corotational approach with a tangent stiffness matrix incorporating matrix $\boldsymbol{K_G}$ which is termed the geometric stiffness matrix, and accounts for changes in geometry as they influence changes in global components of traction [4].

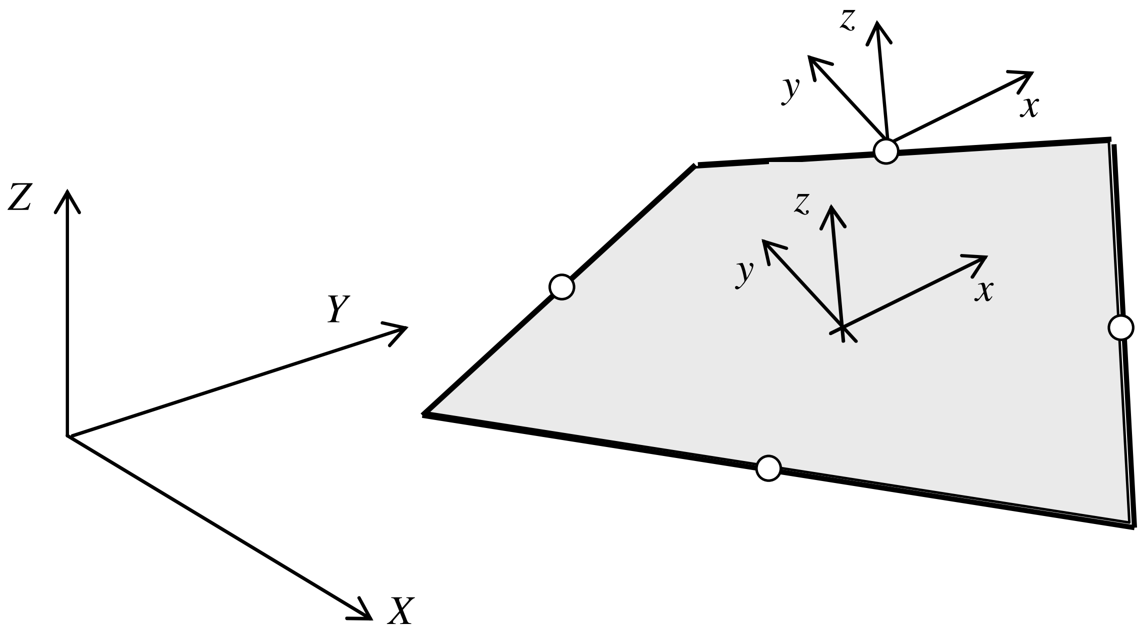

Figure 2: A displaced element with corotated element axes

Then as a first order guide in a Newton-Raphson iterative incremental solution scheme, e.g. with load or arc length control, we utilise the tangent stiffness matrix

$$\boldsymbol{K_T}.\delta\hat{\hat{\boldsymbol{v}}} = \delta\hat{\hat{\boldsymbol{t}}} \text{ with } \boldsymbol{K_T} = \left[\boldsymbol{T^T}\boldsymbol{K}\boldsymbol{T} + \boldsymbol{K_G}\right]$$

where $\boldsymbol{T}$ transforms global components of side displacement to local components.

Although any consistent set of polynomial degrees can be assumed, numerical results are presented based on an element with quadratic moment and rotation fields, linear fields of membrane and transverse shear forces and side translations, and a uniformly distributed load applied in any direction. A strong form of equilibrium is thereby obtained.

Plate bending problem

The first application is to a plate bending problem assuming linear elastic behaviour, and comparisons are made with results from conforming element models where shear locking can occur.

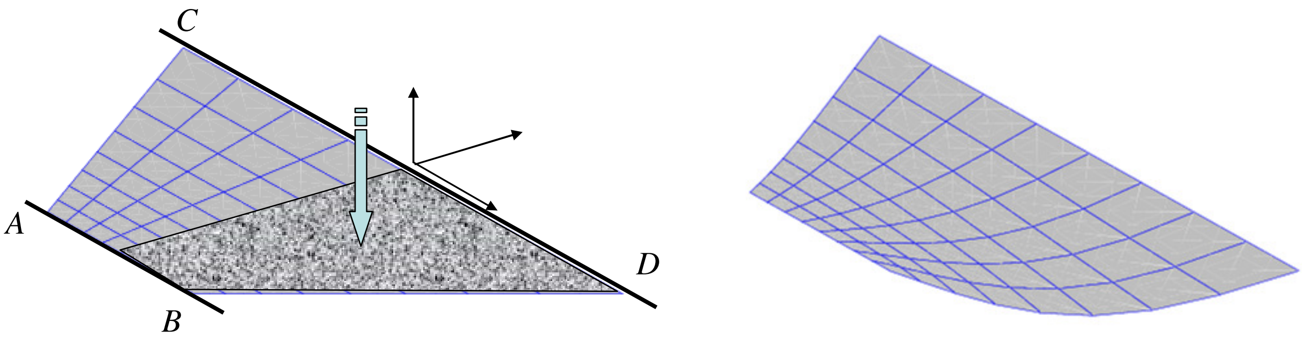

(a) tapered plate with UDL on area indicated (b) deflected form

Figure 3: Plate problem with soft simple supports

The plate shown in Figure 3 spans 8m between lines of support *AB* and *CD* which have lengths 6m and 18m respectively. These supports act as soft simple supports. The mesh shown in Figure 3 is graded in the direction of the span, but elements have uniform dimensions in a direction parallel to the supports. This problem was chosen to require distorted elements which may be more susceptible to locking in conforming models.

The results of linear analyses are plotted as families of graphs in Figure 4. The vertical axis is relative strain energy based on maintaining a constant flexural rigidity by adjusting the value of Young's modulus, and load as the thickness of the plate is reduced. The horizontal axis is log(span/thickness), corresponding to span/thickness in the range 30 to 30,000. Whilst the latter ratio is not encountered in normal civil or mechanical engineering applications, it may be relevant to micro- or nano-scale applications, where a span/thickness of 1000 is not unusual. However, very small thicknesses are considered here mainly in the context of observing the numerical behaviour of the models.

The black and red lines, labelled e32 and e2, at the top of the Figure correspond to hybrid elements used in a fine (32×32) and a coarse (2×2) mesh. As is to be expected, the coarse mesh was the more flexible and had a little more strain energy. There is no evidence of locking as the thickness is reduced, although there is a slight fall in strain energy for very thin plates as the contribution of shear strain energy tends to zero.

However, all the conforming models based on standard 9-noded Lagrange quadrilateral elements exhibited locking as the thickness is reduced. The most extreme form of locking occurred with the 2×2 mesh using 6x6 Gauss integration points (line c2g6), which approximates to full integration. It is interesting to note that locking type solutions with the 2x2 compatible meshes are very similar when (a) the mesh divisions are uniform in the direction of the span and 6x6 integration points per element are used (line c2u6), and (b) the mesh divisions are graded in the direction of the span and

3x3 integration points are used (line c2g3). The implication is that locking is both mesh and numerical integration scheme dependent, and its prediction is problematic.

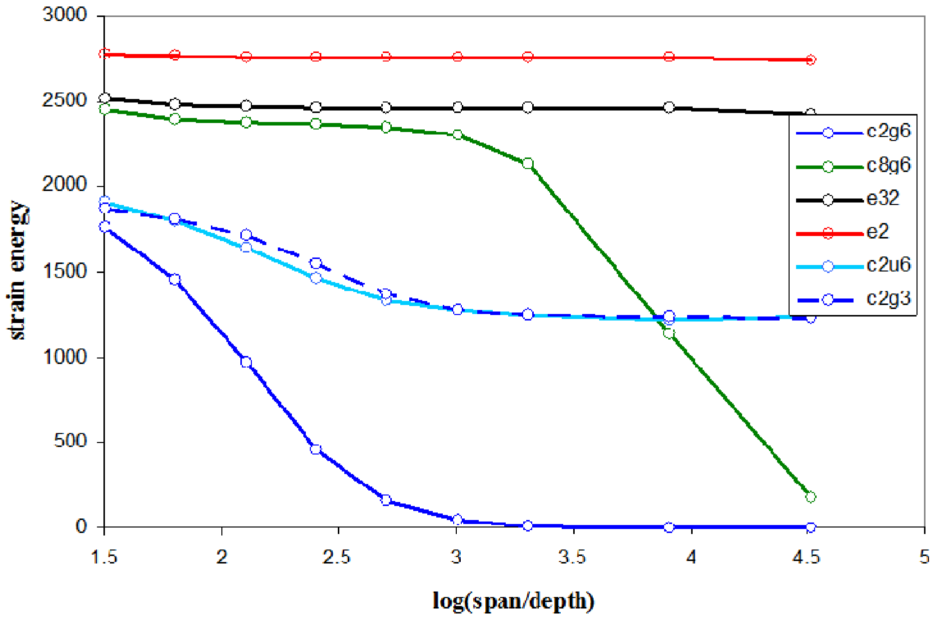

Figure 4: Comparisons of strain energies of plates as thickness varies

It should be noted that of course in practice engineers hopefully would not model the very thin plates indicated in the graphs using Reissner-Mindlin conforming elements!! Kirchhoff elements would then be the more appropriate ones if assumed displacement fields are used [5].

Cylindrical shell problem

The second application is to a cylindrical shell based on the Scordelis-Lo benchmark problem [6]. This is first considered as a linear problem with small displacements, and then as a non-linear problem with large displacements. Figure 5 illustrates a quadrant of the shell with soft simple supports, assumed as from vertical end diaphragms, and a 32×32 mesh of elements. The shell has its longitudinal edges free and it is loaded with a uniform conservative body force, e.g. self-weight. The values of dimensions, loads, and material properties are quoted as for the benchmark problem, and should be assumed to have a consistent set of units.

The normal thickness of the shell is 0.25, and the finite element models are either facetted when using the hybrid flat shell elements with their non-structural corner nodes situated in the mid-surface of the shell, or curved conforming 9-node elements with all nodes situated in the mid-surface. As a benchmark problem, the load value is normally taken as 90, and E = 4.32e8 with Poisson's ratio zero, and linear elastic behaviour is to be assumed.

For the benchmark problem, the hybrid and conforming models with a 32x32 mesh give reliable results for deflection at the midspan of a free edge, to at least 3 significant figures, i.e. δ = 0.302. However it is of interest to consider the non-linear response at this load, since the shell is likely to show significant stiffening when the deflection is of the same order as the thickness! Non-linear analyses to account for deflections with the same models at the load of 90 gave a deflection of 0.254.

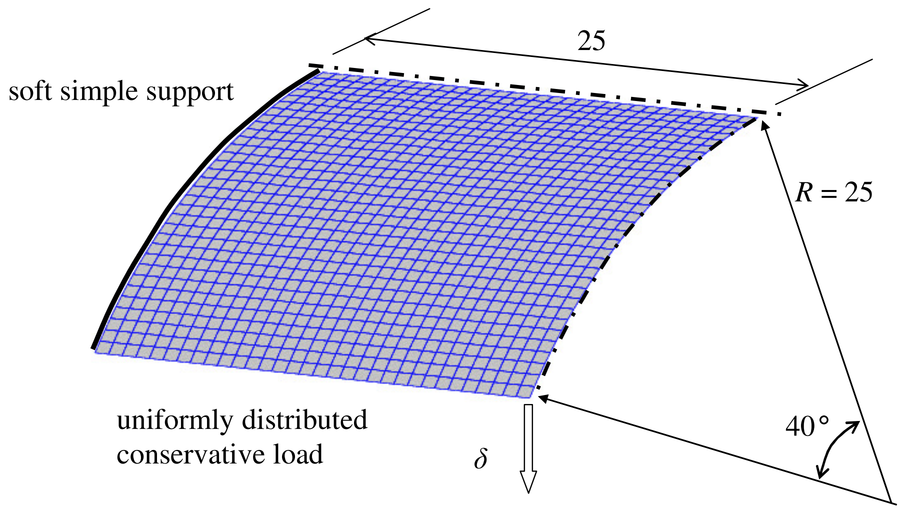

Figure 5: A quadrant of a model of the Scordelis-Lo cylindrical shell

The non-linear behaviour is not usually mentioned, and shows that care should be taken in establishing the reference solutions to benchmark problems. It is also worth noting that there are no results for deflections published in the original ACI paper by Scordelis and Lo [7], only stress-resultants. This seems strange since McNeal & Harder [6], state that Scordelis and Lo published a slightly higher deflection of 0.3086 in the same paper, but in 1969! Confusion reigns on this point. Further results are presented in Figure 6 in order to compare the solutions from different types of model as the thickness is reduced, based on linear elastic behaviour.

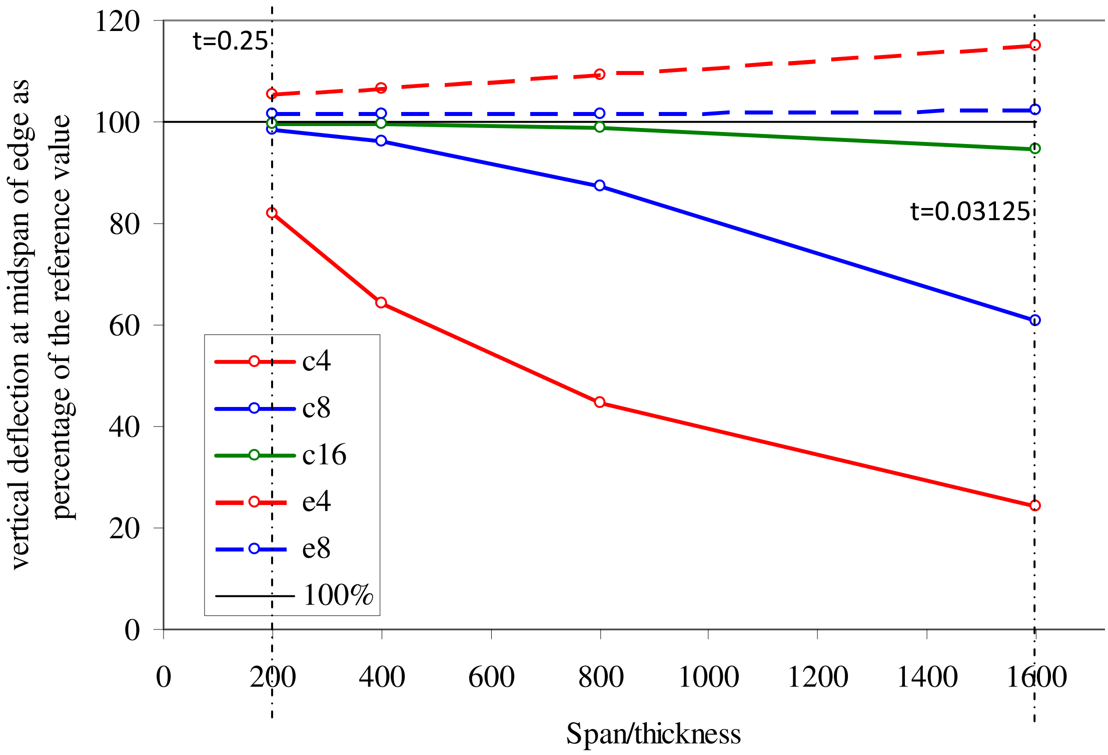

Figure 6: Comparison of linear elastic models with varying span/thickness ratio

In Figure 6 the graphs plot deflection δ at midspan of a free edge, as a percentage of the reference values (obtained from fine mesh models), as the span/thickness ratio increases – with the actual thickness reducing from 0.25 to 0.03125. Each graph corresponds to an $n \times n$ mesh denoted by e*n* or c*n* where “e” or “c” denotes hybrid equilibrium or conforming type of element respectively. All the conforming models again show signs of locking (mainly membrane this time) as the thickness is reduced. The two coarse hybrid models indicate slight reductions in relative stiffness as the thickness is reduced in an apparently linear fashion. This observation has yet to be explained.

Figure 7 shows contour plots of membrane stress-resultants *Nx* in the circumferential direction. Figure 7(a) is derived from the hybrid model and shows smooth variations of forces with small inconsistencies with the expected zero value at the free edge. Figure 7(b) is derived from the conforming model with the same colour coding for contour values as used in Figure 7(a). The black and grey bands indicate where the values are outside the range, and show typical oscillations of membrane stress-resultants based on a 3×3 Gauss numerical integration scheme. This feature may be associated with membrane locking in conforming elements.

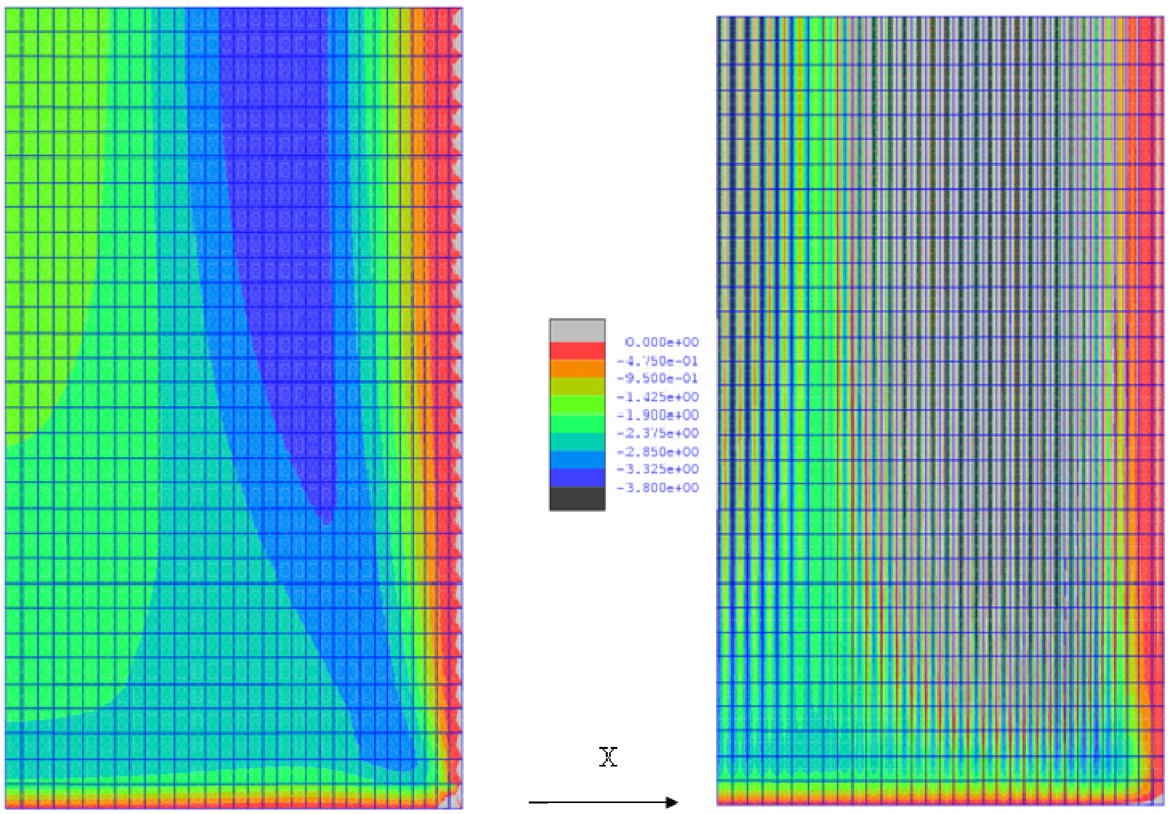

(a) hybrid solution (b) conforming solution

Figure 7: contour plots of membrane stress-resultant *Nx*

Finally the shell models were loaded further to follow the non-linear behaviour due to large displacements. Deflections were measured at 3 points for comparison between different uniform mesh densities as shown in Figure 8.

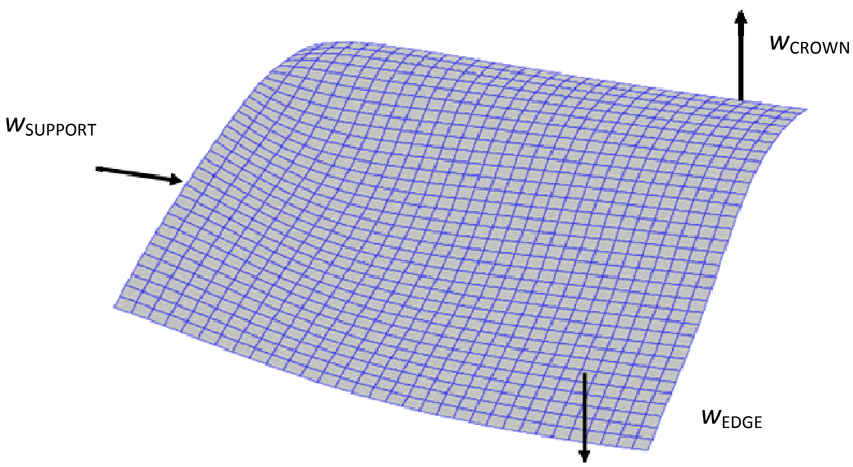

Figure 8: Non-linear behaviour with 3 reference points for deflection

The equilibrium paths for load deflection at these three points are shown in Figure 9, where the vertical Y axis is the UDL normalised at 3000, and the horizontal X axis is the deflection at a point. Each part of Figure 9 contains 4 load/displacement curves – blue for conforming models, red for equilibrium models. 2 meshes are used, a fine mesh of 32x32 elements, and a coarse mesh of 4x4 elements. A sudden change in behaviour occurs at a load of about 1500, after which the supported edge undergoes significant horizontal pull-in (unrestrained at the support – see Figure 9(c)) and the crown point deflection begins to change direction from upwards to downwards – see Figure 9(b). This mode of behaviour, whilst still requiring increasing load, indicates a first mode of buckling.

For the finer mesh, both models agree up to the buckling load, then gradually reveal a distinction, with the hybrid model becoming the stiffer. We have to remember that the compatible model is curved whereas the hybrid model is facetted, and under very large displacements the corotational models become invalid as the elements suffer more extreme deformations. At the load of 1500, the strains due to flexure or membrane actions are of the order of 1%, whereas at the load of 3000, the strains appear to increase to about 2 – 4%, which is borderline for the small strain assumption.

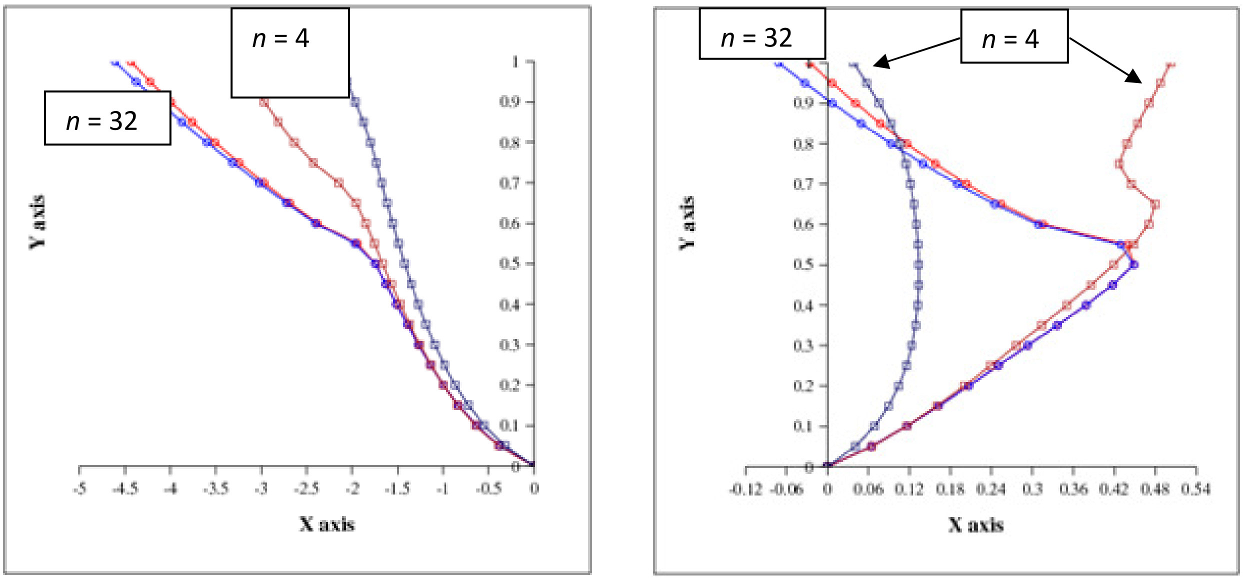

(a) X axis = w_{EDGE} (upwards positive) (b) X axis = w_{CROWN}

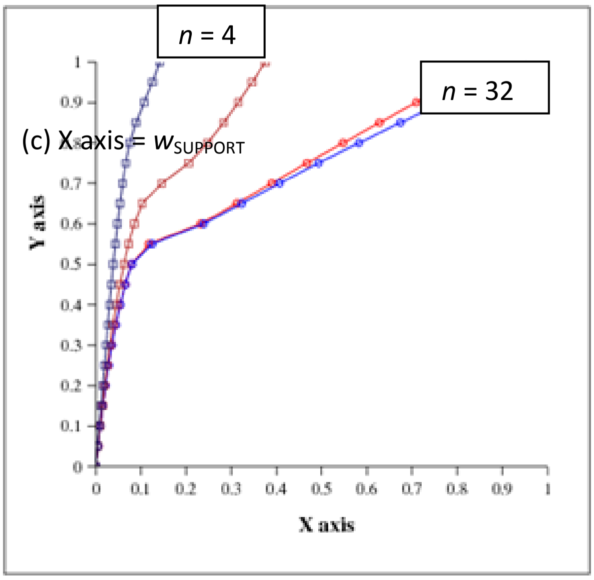

(c) X axis = $w_{SUPPORT}$

Figure 9: Equilibrium load deflection paths

For the coarser mesh the conforming model is significantly overstiff and fails to exhibit the sudden buckling behaviour, whereas the coarser hybrid model does retain reasonable stiffness up to the onset of buckling, albeit at a slightly higher load.

The development of the buckled shape of the cylindrical shell is shown in Figure 10, for the hybrid model, as the load intensity is increased up to 5000. The deflections are plotted at the same scale as the geometry of the original shell. The contour plots shown are for the membrane stress-resultant in the longitudinal (span) direction. The contours are based on different colour codes dependent on the range of their values, consequently they cannot be directly compared for the different loads.

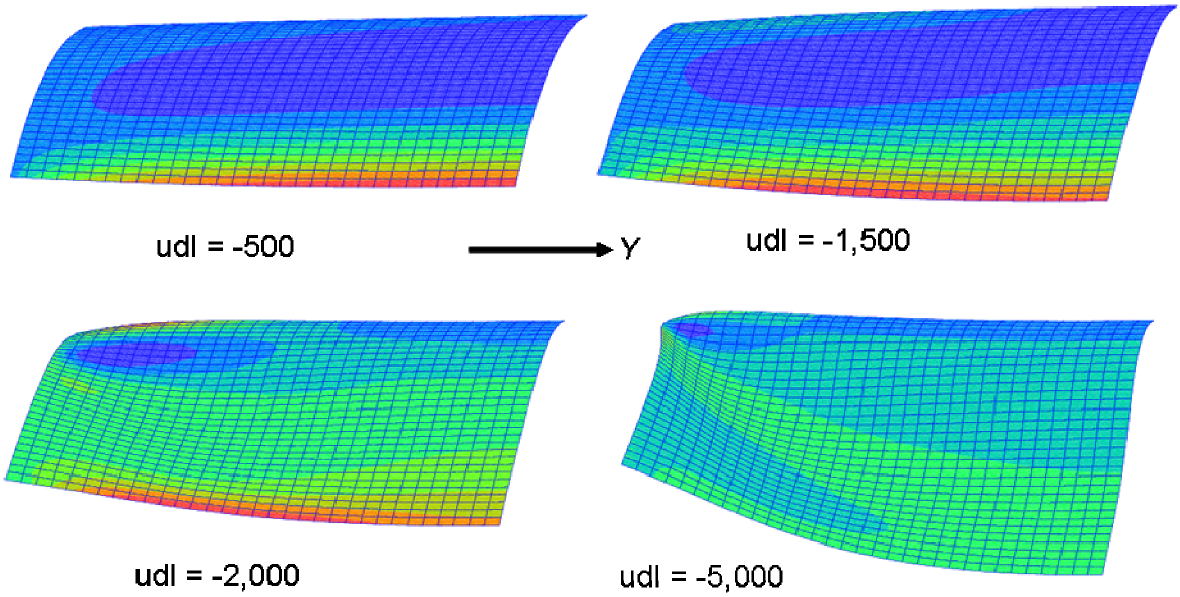

Figure 10: Development of the first mode of buckling together with contours of longitudinal membrane forces

Concluding observations

This article has aimed to demonstrate the quality of results available from finite element models based on quadrilateral hybrid equilibrium elements for both linear and geometrically non-linear behaviours, and to illustrate some of the deficiencies of their more commonly used conforming counterparts.

For practising engineers, the hybrid form of element:

- Interacts via physically meaningful tractions in place of mathematical nodal forces;
- Maintains strong equilibrium both within and between elements;
- Produces good quality side displacements, at least in the pre-buckling range of behaviour;
- Exhibits no locking of displacements for very thin plates;
- Enables solutions from both types of model to be used for error estimation of either model.

References

1. Maunder EAW, Izzuddin BA, An equilibrium approach to finite element modelling of plates and shells, in Proceedings of International Conference on Shells, Plates and Beams, eds. AJM Ferreira, E Viola, F Tornabene, p26, Editrice Esculapio, Bologna, 2015.

2. Izzuddin BA, ADAPTIC User Manual, Imperial College London, 2009

3. Maunder EAW, Almeida JPM, Ramsay ACA, A general formulation of equilibrium macro-elements with control of spurious kinematic modes: the exorcism of an old curse, International Journal for Numerical Methods in Engineering, 39, (18), 3175-3194, 1996.

4. Maunder EAW, Izzuddin BA, A hybrid equilibrium element for folded plate and shell structures, International Journal for Numerical Methods in Engineering, 95, (6), 451-477, 2013.

5. Blaauwendraad J, Plates and FEM, Springer, 2010.

6. McNeal RH, Harder RL, A proposed standard set of problems to test finite element accuracy, Finite Elements in Analysis and Design, 1, 3-20, 1985.

7. Scordelis AC, Lo KS, Computer analysis of cylindrical shells, Journal of the American Concrete Institute, 539-560, 1964.